NAVAL POSTGRADUATE SCHOOL
Monterey, California

THESIS

SPECTRAL ENERGY BALANCE OF WAVES IN THE SURF ZONE

by

Noel R. Russnogle

March, 1998

Thesis Advisor: Thomas H.C. Herbers

Approved for public release; distribution is unlimited.

REPORT DOCUMENTATION PAGE			Form Approved OMB No. 0704-0188

1. AGENCY USE ONLY *(Leave blank)*	2. REPORT DATE March, 1998	3. REPORT TYPE AND DATES COVERED Master's Thesis
4. TITLE AND SUBTITLE Spectral Energy Balance of Waves in the Surf Zone		5. FUNDING NUMBERS
6. AUTHOR(S) Noel R. Russnogle		
7. PERFORMING ORGANIZATION NAME(S) AND ADDRESS(ES) Naval Postgraduate School Monterey CA 93943-5000		8. PERFORMING ORGANIZATION REPORT NUMBER
9. SPONSORING/MONITORING AGENCY NAME(S) AND ADDRESS(ES)		10. SPONSORING/MONITORING AGENCY REPORT NUMBER

11. SUPPLEMENTARY NOTES The views expressed in this thesis are those of the author and do not reflect the official policy or position of the Department of Defense or the U.S. Government.

12a. DISTRIBUTION/AVAILABILITY STATEMENT Approved for public release; distribution is unlimited.	12b. DISTRIBUTION CODE

13. ABSTRACT *(maximum 200 words)*

The spectral energy balance of waves in the surf zone is examined with extensive measurements from the Duck94 experiment. Cross-shore energy flux gradients are estimated from spectra observed with closely spaced pressure sensors. Nonlinear energy exchanges between different wave components in the spectrum are estimated from observed bispectra based on Boussinesq theory for near-resonant triad interactions. Dissipation of wave energy in the poorly understood breaking process is inferred as the residual term in the spectral energy balance.

Analysis of the spectral energy balance shows that large decreases in energy flux observed at the dominant wave frequencies as waves break over a sand bar are closely balanced by nonlinear energy transfers to higher frequencies. That is, the decay of the spectral peak within the surf zone is a result of nonlinear energy transfers rather than direct dissipation. At higher frequencies, observed energy flux gradients are small and do not balance the nonlinear transfers of energy to high frequency components of the spectrum. This analysis suggests that the spectrum is saturated at high frequencies, and thus, the energy that cascades through nonlinear interactions to higher frequencies is dissipated in the high-frequency tail of the spectrum.

14. SUBJECT TERMS Dissipation, Energy Balance, Boussinesq Equations, Ocean Surface Gravity Waves, Nonlinear Interactions, Shoaling, Beach, Energy Flux.			15. NUMBER OF PAGES 42
			16. PRICE CODE
17. SECURITY CLASSIFICATION OF REPORT Unclassified	18. SECURITY CLASSIFICATION OF THIS PAGE Unclassified	19. SECURITY CLASSIFICATION OF ABSTRACT Unclassified	20. LIMITATION OF ABSTRACT UL

NSN 7540-01-280-5500

Standard Form 298 (Rev. 2-89)
Prescribed by ANSI Std. 239-18 298-102

SPECTRAL ENERGY BALANCE OF WAVES IN THE SURF ZONE

Noel R. Russnogle
Lieutenant Commander, United States Navy
B.S., Oregon State University, 1985

Submitted in partial fulfillment
of the requirements for the degree of

MASTER OF SCIENCE IN PHYSICAL OCEANOGRAPHY

from the

NAVAL POSTGRADUATE SCHOOL
March 1998

Author: ______________________
Noel R. Russnogle

Approved by: ______________________
Thomas H.C. Herbers, Thesis Advisor

Edward B. Thornton
Edward B. Thornton, Second Reader

Edward B Thornton for
Robert H. Bourke, Chairman
Department of Oceanography

ABSTRACT

The spectral energy balance of waves in the surf zone is examined with extensive measurements from the Duck94 experiment. Cross-shore energy flux gradients are estimated from spectra observed with closely spaced pressure sensors. Nonlinear energy exchanges between different wave components in the spectrum are estimated from observed bispectra based on Boussinesq theory for near-resonant triad interactions. Dissipation of wave energy in the poorly understood breaking process is inferred as the residual term in the spectral energy balance.

Analysis of the spectral energy balance shows that large decreases in energy flux observed at the dominant wave frequencies as waves break over a sand bar are closely balanced by nonlinear energy transfers to higher frequencies. That is, the decay of the spectral peak within the surf zone is a result of nonlinear energy transfers rather than direct dissipation. At higher frequencies, observed energy flux gradients are small and do not balance the nonlinear transfers of energy to high frequency components of the spectrum. This analysis suggests that the spectrum is saturated at high frequencies, and thus, the energy that cascades through nonlinear interactions to higher frequencies is dissipated in the high-frequency tail of the spectrum.

TABLE OF CONTENTS

ACKNOWLEDGMENT

I express my sincere appreciation to my advisor, Thomas Herbers, for his guidance, patience, and instruction, without which, this paper would never have come about.

I would also like to thank Mike Cook and Paul Jessen, whose code, and assistance in building code enabled me to produce these results. And lastly, to my wife, Elizabeth, for her support and encouragement.

I. INTRODUCTION

The lack of accurate models for the transformation of waves across the surf zone is the greatest deficiency is in our ability to predict surf characteristics (e.g., spilling of plunging breakers), near-shore circulation (e.g., longshore currents, undertow, rip currents), and sediment transport (e.g., beach erosion, accretion and the formation of sand bars). The properties of ocean surface waves on beaches are affected by changes in water depth, the bottom boundary layer, strong nonlinear dynamics in shallow water, and surf zone wave breaking. As the water depth decreases, waves refract towards the beach. As a result, propagation directions in the surf zone are typically close to normal incidence, and the shoaling evolution of waves can be reasonably well described by 1-dimensional models for uni-directional waves.

Turbulence associated with bottom friction causes a gradual decay of waves in shallow water, that is believed to be important to the evolution of wave spectra across shallow continental shelves. On beaches that typically span only O(10) wavelengths, bottom damping is usually neglected. The dominant physical processes that affect wave transformation on beaches are believed to be nonlinear interactions and wave breaking. Nonlinear wave-wave interactions, weak in the open ocean, are strongly enhanced on beaches owing to the weakly dispersive nature of surface gravity waves in shallow water. Energy is continuously exchanged in near-resonant interactions between all triads of wave components with frequencies f_1,f_2,f_3, that obey the interaction rule $f_1 \pm f_2 \pm f_3 = 0$ (*Freilich* and *Guza*, 1984). These so-called triad interactions not only cause a broadening of the wave spectrum (i.e., energy transfers from the dominant waves to higher-and lower frequencies), but are also responsible for the dramatic transformation of wave shapes from nearly symmetric sinusoidal deep water swells to the pitched-forward wave shape of near breaking waves on beaches (*Elgar* and *Guza*, 1985a).

Models for wave shoaling transformation outside the surf zone are usually based on nondissipative Boussinesq equations for weakly nonlinear, weakly dispersive waves (*Peregrine*,1967). These models include time-domain formulations (*Madsen et al.*, 1991), discrete frequency domain formulations (*Freilich and Guza*, 1984; *Liu et al.*, 1985) and

stochastic formulations that predict the evolution of continuous wave spectra (*Herbers and Burton,* 1997; *Norheim et al.,*1998). Extensive comparisons to field data confirm that Boussinesq models predict accurately the shoaling evolutions of waves outside the surf zone (*Freilich and Guza*, 1984; *Elgar and Guza* 1985b; *Norheim et al.*, 1998).

Early surf zone models [*Collins*, 1970; *Battjes*, 1972; *Goda* 1975] simply parameterized the heights of breaking waves in the terms of the local water depth. *Battjes and Janssen* [1978] introduced a frequency-integrated energy balance model with the dissipation sink term based on the energy loss in a turbulent bore and a simple breaking criterium. *Thornton and Guza* [1983] refined this model by incorporating realistic wave height statistics. Extensive comparisons with laboratory and field data for a range of beach profiles and incident wave conditions shows that the energy balance models of *Battjes and Janssen* and *Thornton and Guza* predict accurately the variations of wave heights in the surf zone (*Battjes and Janssen*, 1978; *Thornton and Guza*, 1983; *Battjes and Stive*, 1985). Although wave height decay in the surf zone is predicted accurately by these bulk models for total wave energy, the associated dramatic changes in the wave spectrum resulting from nonlinear interactions are not described by these models, and therefore the characteristics of breaking waves (e.g., spilling vs plunging breakers; narrow vs broad spectra) are not predicted.

Recently, Boussinesq models, that rigorously account for nonlinear interactions, were extended into the surf zone by including a heuristic dissipation term in the shoaling evolution equations (*Mase and Kirby*, 1992; *Kaihatu and Kirby*, 1995; *Eldeberky and Battjes* 1995; *Chen et al.*, 1997). As virtually no information exists on the spectral characteristics of dissipation rates in the surf zone, simple parameterizations were used. *Mase and Kirby*, (1992) and *Kaihatu and Kirby*, (1995) used a frequency dependent dissipation function that combines a constant term that reduces spectral levels uniformly in proportion to the energy at each frequency with a frequency-weighted (f^2) term that dissipates the higher frequency components, using an adjustable coefficient to control the relative importance of the two terms. *Eldeberky and Battjes* (1995) used a frequency independent formulation, in which dissipation is proportional to the energy at each

frequency. *Chen et al.*, [1997] showed that the evolution of wave shapes across the surf zone is predicted more accurately by models with a dissipation term that increases with frequency than models using a frequency independent dissipation term.

To obtain a better understanding of the spectral characteristics of energy dissipation within the surf zone, the spectral energy balance of shoaling and breaking waves is examined in this study using extensive field observations from a natural sandy ocean beach. Neglecting alongshore depth variations, directional spreading of waves and wave reflection from shore, the energy balance can be expressed as

$$F_x(f) = S_{nl}(f) + S_{ds}(f) \tag{1}$$

where the left-hand side is the cross-shore gradient of the energy flux $F(f)$. The source term $S_{nl}(f)$ represents the net nonlinear transfer of energy to waves with frequency f owing to triad interactions. The other source term $S_{ds}(f)$ represents energy dissipation during wave breaking. The energy flux gradients are evaluated from closely spaced instruments.

The energy transfers in near-resonant triad interactions are a function of the phase-relationships between the three interacting components, and thus depend on higher-order statistics of the wave field. A stochastic formulation of the Boussinesq equations yields the following expression for $S_{nl}(f)$ (*Herbers and Burton*,1997; *Norheim et al.*, 1998)

$$S_{nl}(f) = IM\{b(f)\} \tag{2a}$$

$$b(f) = \frac{3\pi f}{h}\{\int_0^f B(f',f-f')df' - 2\int_0^\infty B(f',f)df'\} \tag{2b}$$

where IM{ } indicates the imaginary part. The third-order bispectrum $B(f_1,f_2)$ describes the degree of coupling and the phase relationship in triads of wave components with frequency f_1,f_2 and f_1+f_2 (*Hasselmann et. al.*, 1963). In shallow water, the bispectrum evolves strongly and describes in a statistical sense the shapes of shoaling waves (e.g., *Elgar and Guza,* 1985b; *Elgar et al.*, 1990a). The nonlinear source term $S_{nl}(f)$ in the energy balance involves an integral $b(f)$ of $B(f_1,f_2)$ over all triads that include a component with frequency f.

In the present study the terms in the energy balance equation (1) were examined with measurements from a cross-shore array of pressure sensors deployed near Duck N.C., in 1994. The energy flux gradient $F_x(f)$ and nonlinear source term $S_{nl}(f)$ were estimated from measured spectra and bispectra at 14 cross-shore positions. The associated dissipation rate $S_{ds}(f)$ was then inferred as the residual term in equation 1. The field data and analysis are described in section 2.

Example observations of the energy balance in a range of conditions are presented in section 3, followed by a statistical analysis of the entire 2 months observations in section 4. In the surf zone, large negative values of $F_x(f)$ in the energetic part of the spectrum are shown to be approximately balanced by $S_{nl}(f)$. These results show that the energy of the dominant waves is not directly dissipated in the surf zone, but transferred to higher frequencies through nonlinear interactions where the energy is presumably dissipated. The results are summarized in section 5.

II. FIELD DATA AND ANALYSIS

Detailed field measurements of the evolution of shoaling and breaking waves on a natural ocean beach were acquired during the Duck 94 experiment at the U.S. Army Corps of Engineer Field Research Facility located near Duck, N.C., on a relatively straight barrier island exposed to the open Atlantic ocean. A dense cross shore transect of 14 pressure sensors was deployed, extending from the shore line to about 5 m depth (350 m from shore)(Figure 1). Collocated with each pressure sensor was a sonar altimeter that provided accurate estimates of the location of the sea floor. The sample frequency of all sensors was 2 Hz. High quality data were collected nearly continuously during the months of September and October 1994 (*Elgar et al.*, 1997).

The closely spaced pressure sensors allowed for direct estimates of the advection term $F_x(f)$ and the nonlinear source term $S_{nl}(f)$ in the energy balance equation (1). A surface elevation spectrum $E(f)$ and bispectrum $B(f_1,f_2)$ with resolution of .0078 Hz were estimated from each hour-long pressure record using the shallow water approximation.

The spectral energy balance was evaluated at the midway point between adjacent instruments using a simple finite difference approximation. The energy flux gradient $F_x(f)$ was approximated by (using the shallow water approximation of the group speed):

$$F_x(f) \approx \frac{E_2(f)(gh_2)^{\frac{1}{2}} - E_1(f)(gh_1)^{\frac{1}{2}}}{x_2 - x_1} \tag{3}$$

where $x_1, x_2 (>x_1)$ are the cross-shore positions of a pair of adjacent sensors, h_1 and h_2 are the corresponding water depths, $E_1(f)$, and $E_2(f)$ are the corresponding spectra.

The nonlinear energy transfer term (S_{nl}) at the same midway point was approximated by:

$$S_{nl}(f) = \frac{1}{2}\{b_1(f) + b_2(f)\} \tag{4}$$

with $b_1(f)$ and $b_2(f)$ the bispectral integral b(f)(Eq.2b) evaluated at the instrument locations x_1 and x_2.

Significant weather changes throughout the Duck 94 experiment provided ample sampling of a multitude of surf conditions including two major Noreaster storms with maximum significant wave heights of 2.5 m and 3.8 m (Figure 2) and surf zones extending across the entire instrumented transect. The data set also includes calm periods with significant wave heights as small as .2 m and virtually no breaking across the transect. Observed wave spectra include narrow spectra of long period, remotely generated swells, broad spectra of locally generated seas and mixed swell-sea spectra. The bottom profile during the experiment consisted of a mild offshore slope with a well developed bar approximately 100 m from shore followed by a trough and steeper foreshore. (Figure 1). Fluctuations of bottom topography in the surf zone were minor throughout the data collection period with the exception of the passage of the largest storm that moved the bar 80 meters seaward.

III. OBSERVED SPECTRAL ENERGY BALANCE

The spectral energy balance of shoaling and breaking waves observed for a wide range of conditions is illustrated here with four case study examples (Figure 2), each based on a 1-hour long data record. For each case, the evolution of the spectrum E(f) across the beach is shown in Figure 3, and a representative video image of the sea surface in the instrumental area is shown in Figure 4. In case I, small amplitude swell propagated across the instrumented transect with little breaking (Figure 4). The evolution of the narrow spectrum shows the expected growth of harmonic peaks. Breaking and associated energy losses occurred primarily on the beach face shoreward of instrument array (Figure 4).

Case studies II and III are from the two major storm that passed through the region during the experiment. In both cases the irregular surf zone with spilling breakers extended across the entire 350m-long transect (Figure 4). The evolution of the spectra of these broad wind seas across the surf zone is similar with a strong, nearly uniform decay of spectral levels in the energetic part of the spectrum (Figure 3). In case IV, during the waning of the second Noreaster, moderately energetic swell was observed. This case is characterized by a narrow surf zone confined to the inner part of the instrument array, with some intermittent breaking occurring farther offshore on the sand bar (Figure 4). The spectra observed in case IV indicate a pronounced second harmonic peak outside the surf zone. Inside the surf zone both the primary spectral peak and the second harmonic peak are attenuated.

To examine the role of nonlinear interactions and dissipation processes in the observed spectral evolution of these four case studies, estimates of the energy flux gradient $F_x(f)$ (Eq. 3) and the nonlinear transfer $S_{nl}(f)$ (Eq. 4) are compared in Figures 5-8. The dissipation term $S_{ds}(f)$in the energy balance can be inferred as the difference between the estimated $F_x(f)$ and $S_{nl}(f)$ (Eq. 1). In the non-breaking wave Case I (Figure 5) the observed values of S_{nl} and F_x are approximately equal at all locations except for the innermost two, indicating that the observed spectral changes (Figure 3) are the result of nonlinear energy exchanges, consistent with Boussinesq model results for similar

conditions presented in *Elgar et al.*, (1997) and *Norheim et al.*, (1998). The positive values of S_{nl} and F_x in the range 0.1-0.4 Hz indicate a transfer of energy from the dominant 0.07 Hz swell to high-frequency harmonic components, consistent with the Boussinesq model predictions of *Elgar et al.* (1997) and *Norheim et al.,* (1998). The largest transfers occur slightly inshore of the bar crest (H,I) and on the beach face (L). Comparisons of F_x and S_{nl} at low frequencies (<0.1 Hz) are not shown because partial reflection of the small amplitude swell from the beach face (Elgar et al., 1997), caused large errors in the energy flux estimates (i.e., standing wave nodes and antinodes). Reflection effects are apparent in the large fluctuations of F_x observed at the innermost stations K and L (Figure 5).

In case II with energetic seas breaking across the entire transect (Figure 6), the S_{nl} estimates are characterized by a negative lobe centered at the spectral peak frequency, and a broader positive lobe at higher frequencies. The integral of $S_{nl}(f)$ over all frequencies is zero because the triad interactions conserve energy. The S_{nl} estimates show that energy is primarily transferred from the energetic part of the spectrum to higher frequencies. The observed energy transfer increases from the outer most station C (A and B were not operational during this event) to a maximum value on the sand bar crest (F) decreasing to small values near the shoreline (i.e., where most of the energy has been dissipated). The estimated energy flux gradients F_x show a negative lobe in the energetic part of the spectrum that nearly equals the negative lobe in the S_{nl} estimates. The surprisingly close balance of F_x and S_{nl} demonstrates that the large energy losses observed in the energetic part of the spectrum (Figure 3) are accounted for by nonlinear transfers to higher frequencies, and thus no significant dissipation takes place in the energetic part of the spectrum.

The observed energy flux gradients and nonlinear transfers do not balance at higher frequencies. Whereas $S_{nl}(f)$ estimates show a broad positive lobe above the spectral peak frequency, the associated $F_x(f)$ estimates are close to zero. These results suggest that the energy transferred through nonlinear interactions to higher frequencies cannot be absorbed in the high-frequency tail of the spectrum and is presumably dissipated,

qualitatively consistent with the saturation of wave spectra in the surf zone observed by *Thornton* (1977, 1979). In the most energetic Case III, similar fully developed seas with a lower peak frequency (.09 Hz) were observed (Figures 3,4). In this severe storm, several instruments failed and thus the energy balance could not be evaluated on the seaward side of the bar crest. Nevertheless the estimates of $S_{nl}(f)$and $F_x(f)$ (Figure 7) are remarkably similar to the case II estimates, with a close balance between energy losses in the energetic part of the spectrum (the negative lobe of $F_x(f)$)and energy transfers to higher frequencies (the negative lobe of $S_{nl}(f)$), and an apparent saturation of the spectrum at high frequencies ($S_{nl} > 0$ and $F_x \approx 0$). As in Case II the largest energy transfers are observed at station F on the bar crest. At the innermost stations K and L, fluctuations in $F_x(f)$ at lower frequencies indicate that wave reflection from the steep beach face (i.e., nodes and antinodes) caused significant errors in the energy flux estimates.

A few days later (Case IV) the storm has moved offshore and swell with a peak frequency of 0.09 Hz (Figure 3) propagated though the array. Seaward of the bar crest at stations A and B energy is transferred from the spectral peak to it's secondary harmonic and higher frequencies (Figure 8). The negative values of F_x observed at station B do not balance the positive S_{nl} estimates, suggesting some energy is dissipated. No data was collected on the bar crest but the large reduction in spectral levels between stations B and F (Figure 3) indicates strong dissipation takes place in intermittent wave breaking on the bar crest. Between the bar and the beach face at stations F-J, nonlinear energy transfers are approximately balanced by the estimated energy flux gradients. Whereas at station F, energy is transferred from the primary peak to the 2nd harmonic, further inshore at stations I and J energy is transferred from the second harmonic to higher frequencies. Finally, at the shallowest stations K and L located well inside the surf zone, the S_{nl} estimates show large transfers of energy from the energetic part of the spectrum to higher frequencies. As in cases II and III, the F_x estimates closely balance S_{nl} in the energetic part of the spectrum, and $F_x \approx 0$ at high frequencies, indicating that the decay of the energetic part of the spectrum results from nonlinear transfers to the saturated high-frequency tail of the spectrum where the energy is dissipated.

IV. DISCUSSION

The nonlinear transfer of energy to or from wave components with frequency f is controlled by the phase $\theta(f)$ of the bispectrum integral b(f) (Eq. 2). In intermediate water depths (kh=O(1)) the theoretical value of this so called biphase is 0^0 or 180^0 (Hasselmann et al., 1963). For $\theta = 0$ or 180^0, the imaginary part of $b(f) = 0$ and thus no transfers of energy take place. At these depths the bispectrum describes the nonresonant coupling between the primary wind waves and bound secondary waves. In shallow water (kh<<1) biphases evolve allowing for energy transfers in near-resonant triad interactions. Negative biphase values correspond to a loss of energy for components with frequency f, and positive values ($0<\theta(f)<180^0$) indicate energy gains. The biphase θ also characterizes the shape of waves that typically evolve from symmetric profiles in deep water (θ=0 or 180^0) to pitched-forward crests prior to breaking in shallow water ($\theta = \pm 90^0$) (*Elgar and Guza*, 1985).

Biphase estimates are shown in Figure 9 for all four case studies at locations: seaward of the bar, near the bar crest, and on the beach face. Seaward of the bar, the biphases are close to the intermediate depth values 0^0 or 180^0. Case I shows more scatter probably because the nonlinearity is weak in this case and thus the bispectral estimates have greater statistical uncertainty. Near the bar crest, the bisphases have evolved in cases I-III to about 135^0 near the peak frequency and to $30\text{-}90^0$ at higher frequencies. The strongest asymmetry is observed in the non-breaking Case I where θ is close to 90^0 at the second harmonic peak frequency. Interestingly in cases I-III biphases observed on the beach face show a relaxation towards the values 0 and 180^0 for symmetric wave profiles. On the other hand, in case IV biphases observed inshore of the bar crest (where waves reform after breaking on the bar) are close to 0 and 180^0, and strong asymmetry does not develop until waves break again on the beach face. These results indicate that asymmetries in wave profiles are most pronounced during or before the onset of wave breaking and disappear in the inner region of wide surf zones.

The energy balance observed in case studies II-IV with energetic breaking waves (i.e., the surf zone extends seaward of the sand bar) is qualitatively similar with nonlinear

interactions transferring energy from the energetic part of the spectrum to higher frequencies where the energy is dissipated. This surf zone balance is shown in Figures 10 and 11 to hold for all observations with an energetic wide surf zone during the two month long experiment. Only 77 low-tide observations with incident wave variances measured in 8 m depth > 2000 cm^2 (i.e., significant wave heights > 1.8 m) are included to restrict the comparisons to wide surf zones that extend across the entire instrumented transect. Estimates of $F_x(f_p)$ and $S_{nl}(f_p)$ at the spectral peak frequency (f_p) are compared at locations A-L(midway between adjacent instruments) in Figure 10.

Between the seaward end of the transect and slightly inshore of the bar crest (locations A-I), $S_{nl}(f_p)$ and $F_x(f_p)$ are both negative and approximately equal. Correlation coefficients between S_{nl} and F_x vary between .76-.96 with least-squares fit lines that are close to (within 5-30%) a one-to-one correspondence. These estimates demonstrate that the large energy losses observed in the surf zone at the spectral peak frequency are accounted for by nonlinear transfers to higher frequencies rather than direct dissipation of wave energy in the energetic part of the spectrum.

Close to shore (locations J-L) the $S_{nl}(f_p)$ estimates are small and in poor agreement with $F_x(f_p)$ estimates. At these inner surf zone locations, energy levels may be reduced enough that significant reflected components from the beach (e.g., an antinode near the shoreline) contribute large errors to the energy flux gradient $F_x(f_p)$ estimates (e.g., the large positive $F_x(f_p)$ estimates at L).

To characterize the energy balance at higher frequencies, the $S_{nl}(f)$ and $F_x(f)$ integrated over the frequency range of .3-.5 Hz are compared in Figure 11. Whereas the S_{nl} estimates show consistently positive values (i.e., energy transfers to high frequencies, F_x estimates are comparatively small. These results confirm that the high-frequency tail of the spectrum is saturated in the surf zone and the energy transferred to high frequencies in nonlinear interactions is immediately dissipated. The largest energy transfers (and hence dissipation rates) are observed at stations F-L, near the crest of the sand bar, and L on the beach face where the strongest breaking activity is expected.

V. SUMMARY AND CONCLUSIONS

The spectral energy balance of shoaling and breaking waves was examined with two months of field observations from a 350m-long cross-shore transect of 14 pressure sensors deployed on a barred ocean beach near Duck, NC as part of the Duck 94 Experiment (*Elgar et al.*, 1997). The energy flux gradient term $F_x(f)$ and the nonlinear source term $S_{nl}(f)$ in the energy balance equation were estimated at 13 cross shore positions from approximately 1400 hour-long pressure records. The energy flux gradient $F_x(f)$ was estimated from the measured changes in the wave spectrum $E(f)$ between two adjacent instruments. The net nonlinear energy transfer $S_{nl}(f)$ resulting from near-resonant triad interactions was estimated from the observed wave bispectrum $B(f_1,f_2)$ based on a stochastic Boussinesq model (*Herbers and Burton*, 1997).

In low-energy conditions, when waves propagate across the instrumented transect with little or no breaking, the observed small nonlinear energy transfers to higher frequencies are approximately balanced by the growth of the spectrum at high frequencies, consistent with earlier studies *Elgar et al.*(1997), *Norheim et al.*(1998). In high-energy conditions with waves breaking across the entire transect, the $S_{nl}(f)$ estimates consistently show a large negative lobe at the spectral peak frequency and a broad positive lobe at higher frequencies, consistent with a strong nonlinear transfer of energy from the spectral peak to a broad range of higher frequencies. The largest energy exchanges are observed on the crest of the sand bar, where wave breaking is most intense. The observed negative energy flux gradients in the energetic part of the spectrum closely balance the nonlinear transfers. Theses observations show that the large energy losses in the spectral peak of breaking waves are accounted for by nonlinear transfers to higher frequencies, and thus

no significant dissipation occurs in the energetic part of the spectrum. At higher frequencies the observed F_x are small and do not balance the positive S_{nl} values. These results support earlier observations (*Thornton*, 1977, 1979) that wave spectra in the surf zone are saturated at high frequencies (i.e., energy transferred through nonlinear interactions cannot be absorbed in the high-frequency tail of the spectrum and is presumably dissipated).

In conclusion, the present observations of the spectral energy balance in the surf zone show that near-resonant triad interactions transfer energy from the energetic part of the wave spectrum to higher frequencies where the energy is dissipated.

APPENDIX

Figure 1. Instrument locations in the Duck94 experiment. Squares indicate the 14 cross-shore positions of a co-located pressure sensor and sonar altimeter. A (outermost) through M (innermost) indicate the midway points between adjacent instruments.

Figure 2. Variability of incident wave variances estimated in the frequency range 0.05-0.25 Hz from bottom pressure measurements in 8 meter depth (instruments deployed and maintained by the U.S. Army Corps of Engineers) using a linear theory depth correction. Hourly variance estimates are shown versus time for the two months of continuous data collected. Dotted vertical lines denote the four case studies analyzed in section 3.

Figure 3. Observed shoaling evolution of wave spectra in the four case studies. In each case spectra at four locations spanning the transect (Figure 1) are shown.

Figure 4. Representative surf zone photographs (courtesy of T.C. Lippmann) of four case studies obtained with video cameras mounted on a nearby tower about 50 m above the sea surface. The top, middle-left and lower-left photographs all cover the same area including the inner half of the instrumented transect (solid line). The middle-right and bottom-right photos provide simultaneous, slightly overlapping (≈20m) images that cover the outer half of the instrumented transect (solid line). The outward looking camera was not operational during cases I and II.

Figure 5. Estimates of the energy flux gradient $F_x(f)$(dot-dash) and the nonlinear

transferred energy $S_{nl}(f)$ (solid) versus frequency f at 10 cross-shore locations in case study I. The beach profile and the cross-shore locations where the energy balance is evaluated are indicated in the bottom right panel. Arrows indicate the spectral peak frequency.

Figure 6. Estimates of $F_x(f)$ and $S_{nl}(f)$ in Case study II at 10 cross-shore locations (same format as figure 5).

Figure 7. Estimates of $F_x(f)$ and $S_{nl}(f)$ in Case study III at 8 cross-shore locations (same format as figure 5).

Figure 8. Estimates of $F_x(f)$ and $S_{nl}(f)$ in Case study IV at 9 cross-shore locations (same format as figure 5).

Figure 9. Biphase θ versus frequency f (Hz) seaward of the bar, near the bar crest, and on the beach face. From top to bottom: case I at locations C,G,L, case II at C,G,L, case III at A,F,L, and case IV at A,F,L,.

Figure 10. Nonlinear energy transfer S_{nl} versus the energy flux gradient F_x at the spectral peak frequency in energetic surf zone conditions. Each scatter diagram shows the comparison at one cross-shore location (comparisons at locations D and E where only few observations were collected are not shown). Each dot represents an estimate based on a 1-hour-long data record. A linear regression line (dash-dot) and correlation coefficient between F_x and S_{nl} are indicated in each scatter diagram. For reference, a representative beach profile with the instrument locations is shown in the lower right panel.

Figure 11. Nonlinear energy transfer S_{nl} versus the energy flux gradient F_x, both integrated over the high-frequency range 0.3-0.5 Hz, in energetic surf zone conditions

(same format as figure 10).

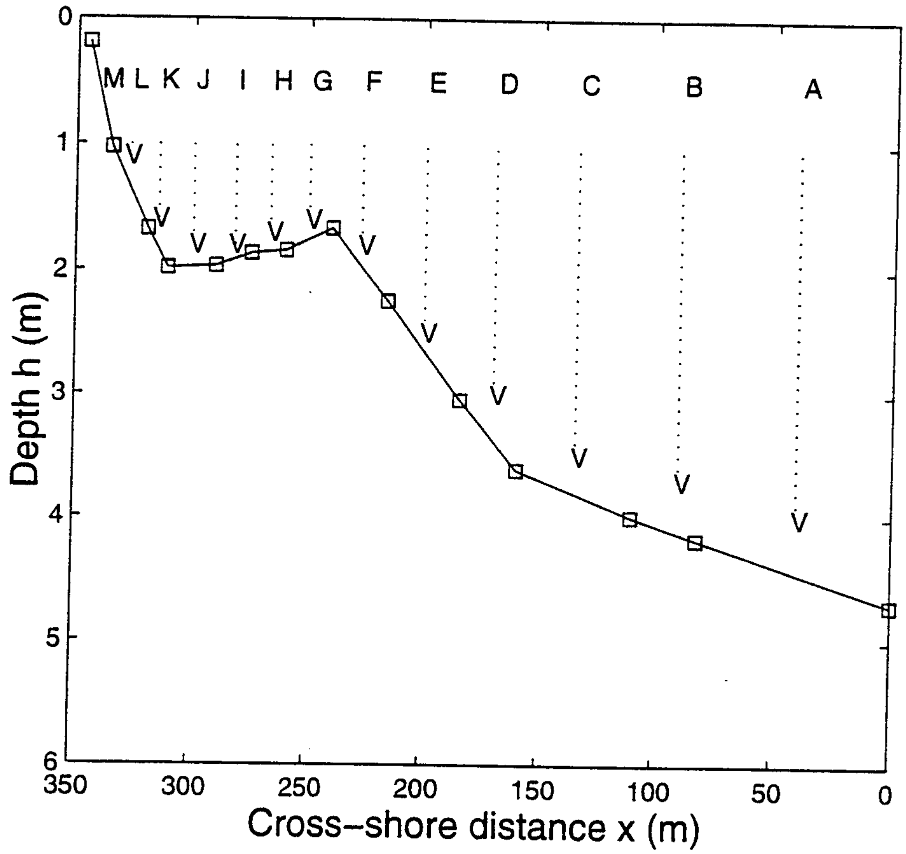
M L K J I H G F E D C B A
V
Depth h (m)
0
1
2
3
4
5
6
350
300
250
200
150
100
50
0
Cross–shore distance x (m)

Figure 1

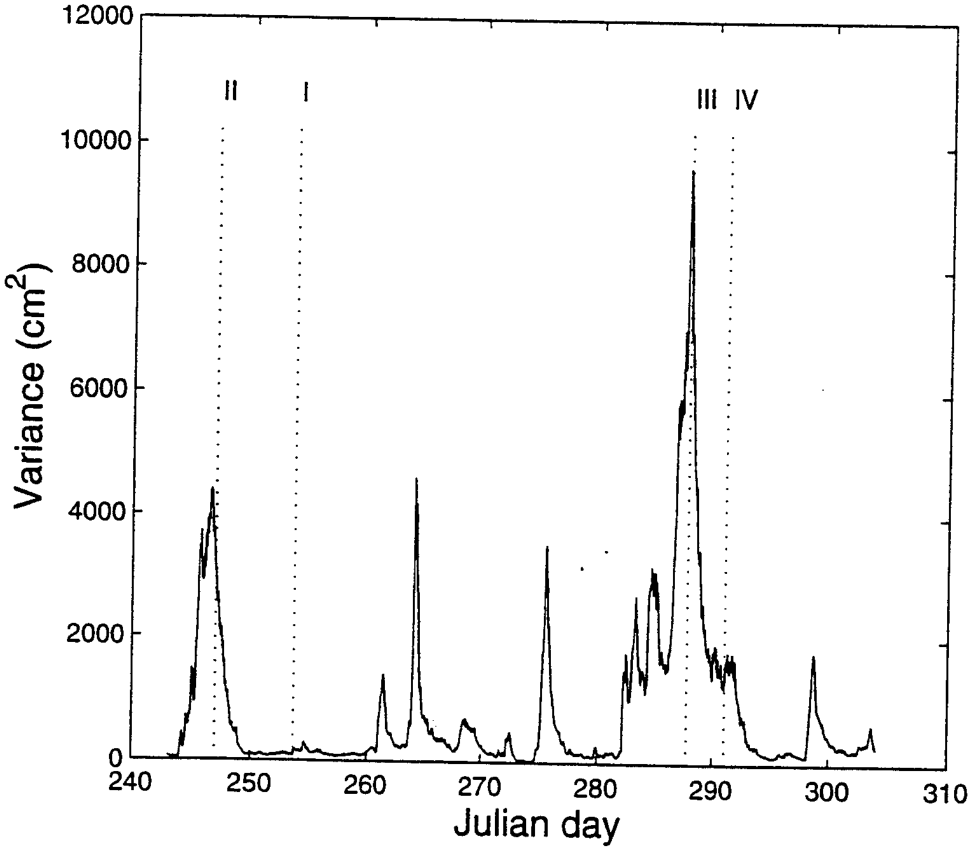

12000
10000
8000
6000
4000
2000
0
240
250
260
270
280
290
300
310
Variance (cm^2)
Julian day
II
I
III
IV

Figure 2

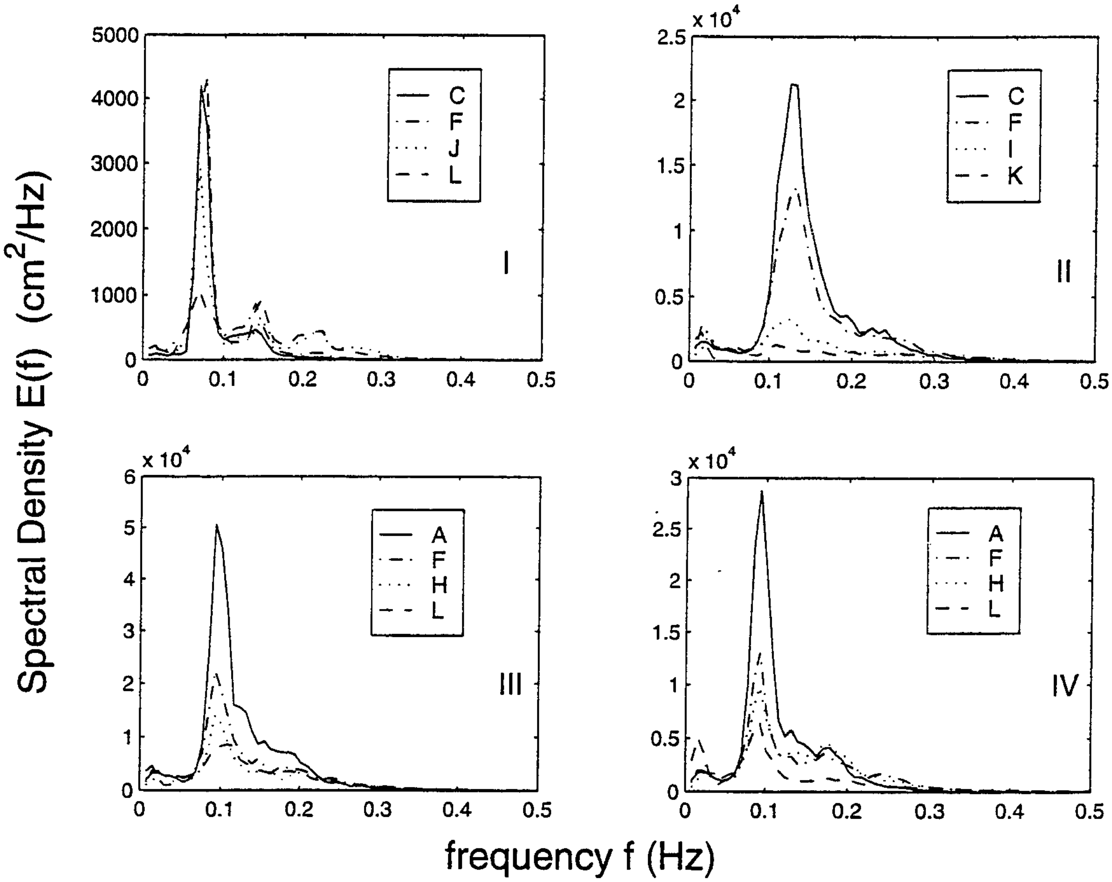

Spectral Density E(f) (cm²/Hz)
frequency f (Hz)
5000
4000
3000
2000
1000
0
0.1
0.2
0.3
0.4
0.5
C
F
J
L
I
x 10⁴
2.5
2
1.5
1
0.5
C
F
I
K
II
x 10⁴
6
5
4
3
A
F
H
L
III
x 10⁴
3
2.5
A
F
H
L
IV

Figure 3

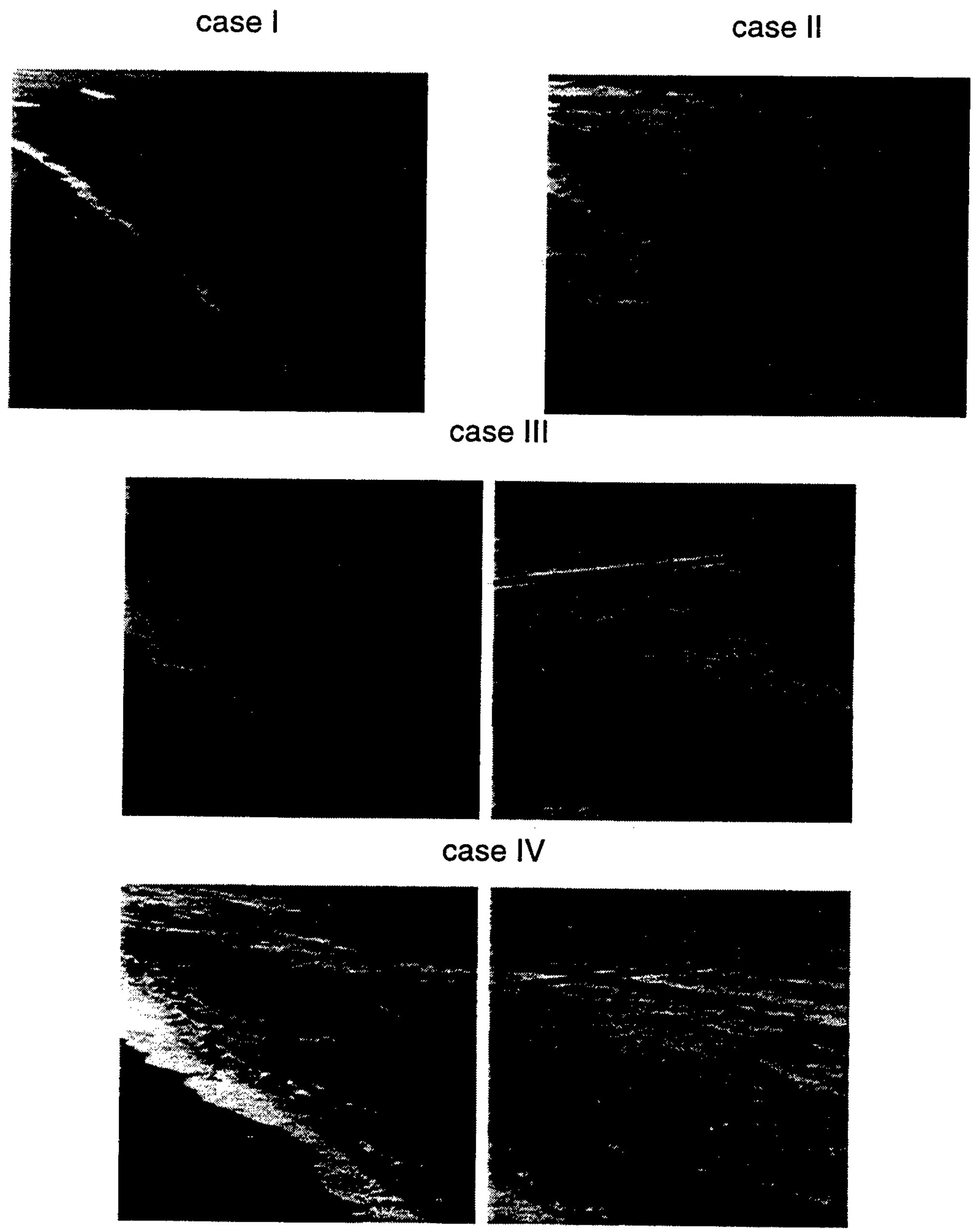

Figure 4

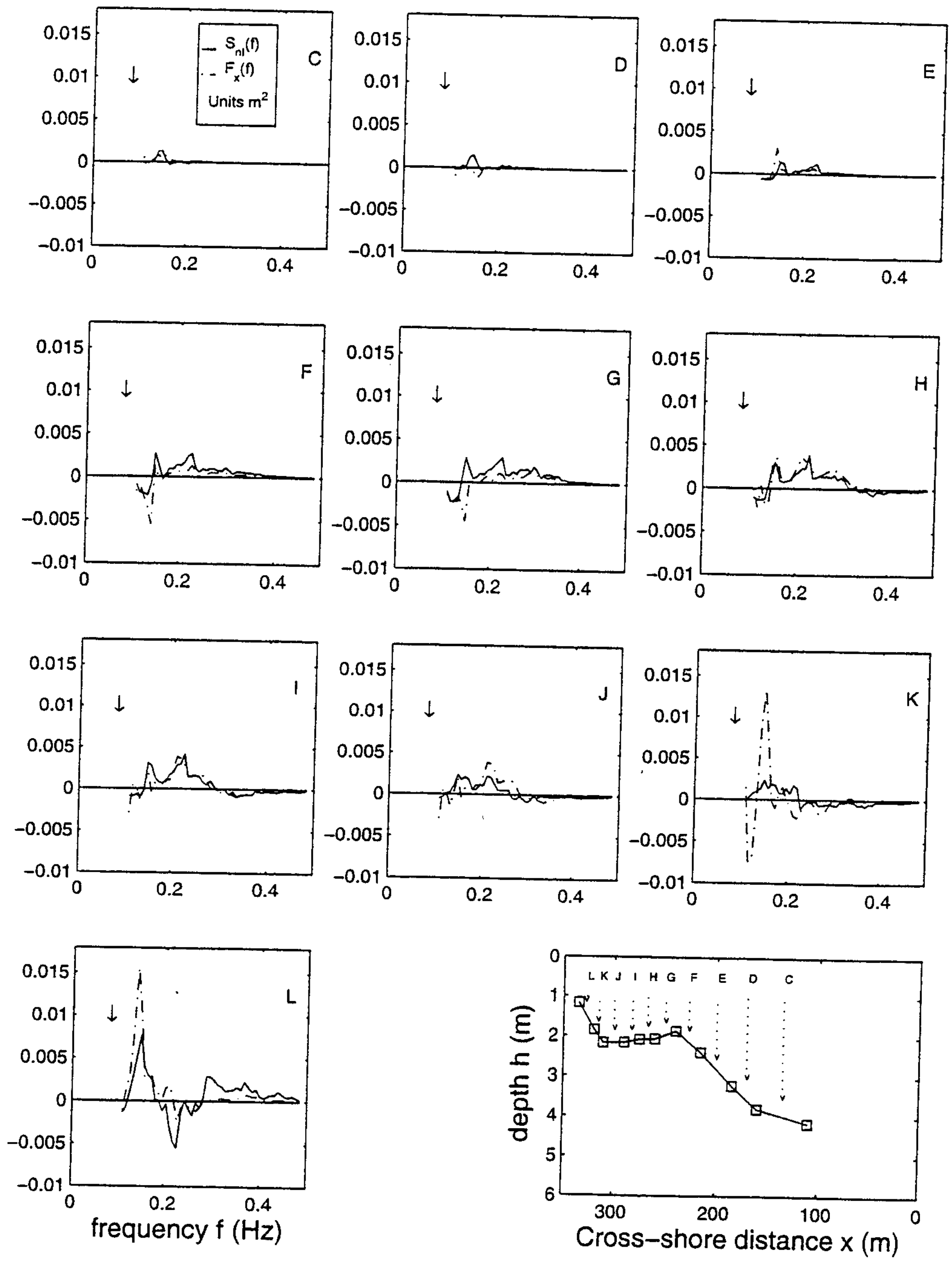

$S_{nl}(f)$
$F_x(f)$
Units m^2
C
D
E
F
G
H
I
J
K
L
frequency f (Hz)
depth h (m)
Cross-shore distance x (m)
L K J I H G F E D C

Figure 5

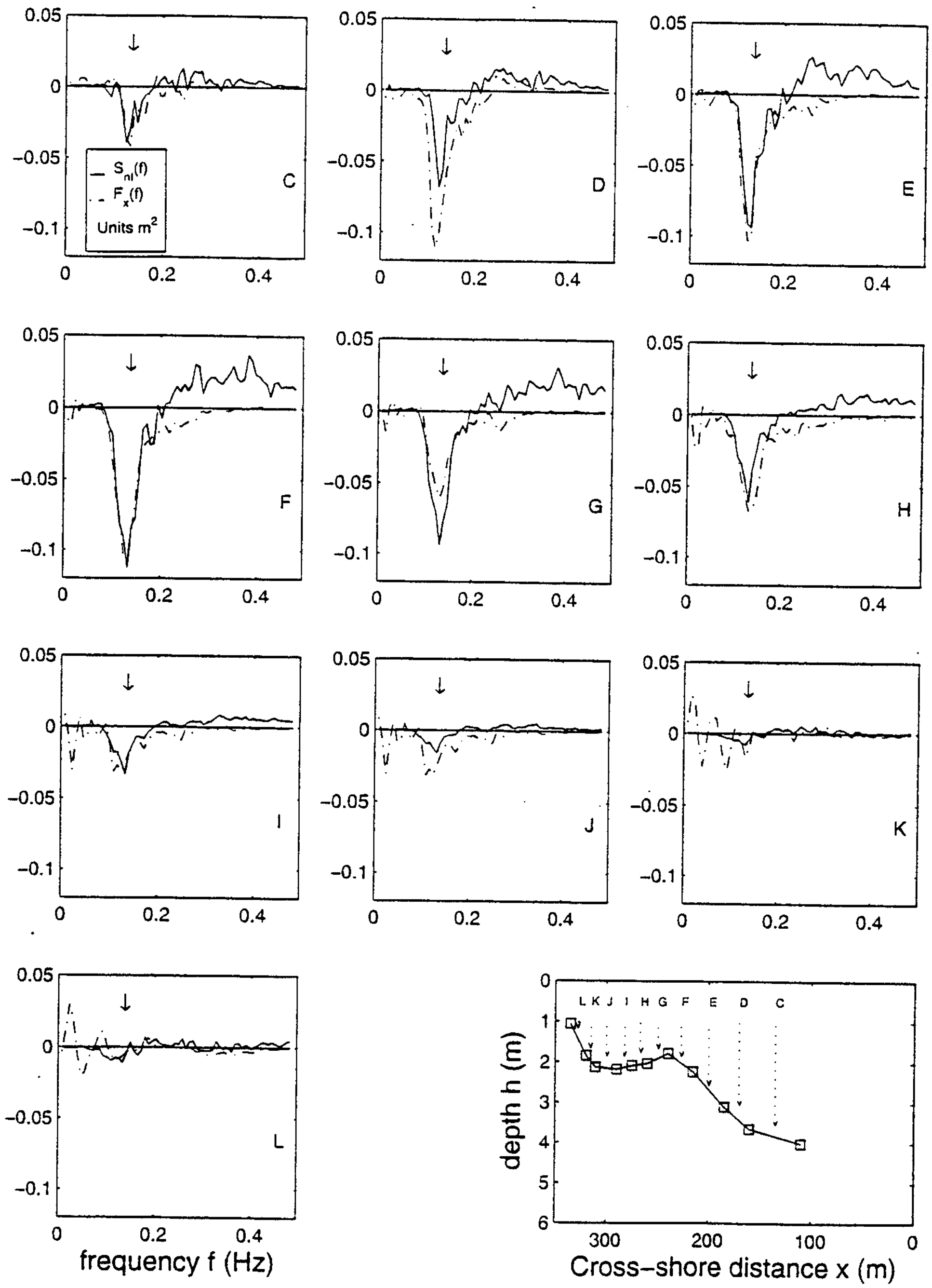

$S_{nl}(f)$
$F_x(f)$
Units m²
C
D
E
F
G
H
I
J
K
L
frequency f (Hz)
L K J I H G F E D C
depth h (m)
Cross-shore distance x (m)

Figure 6

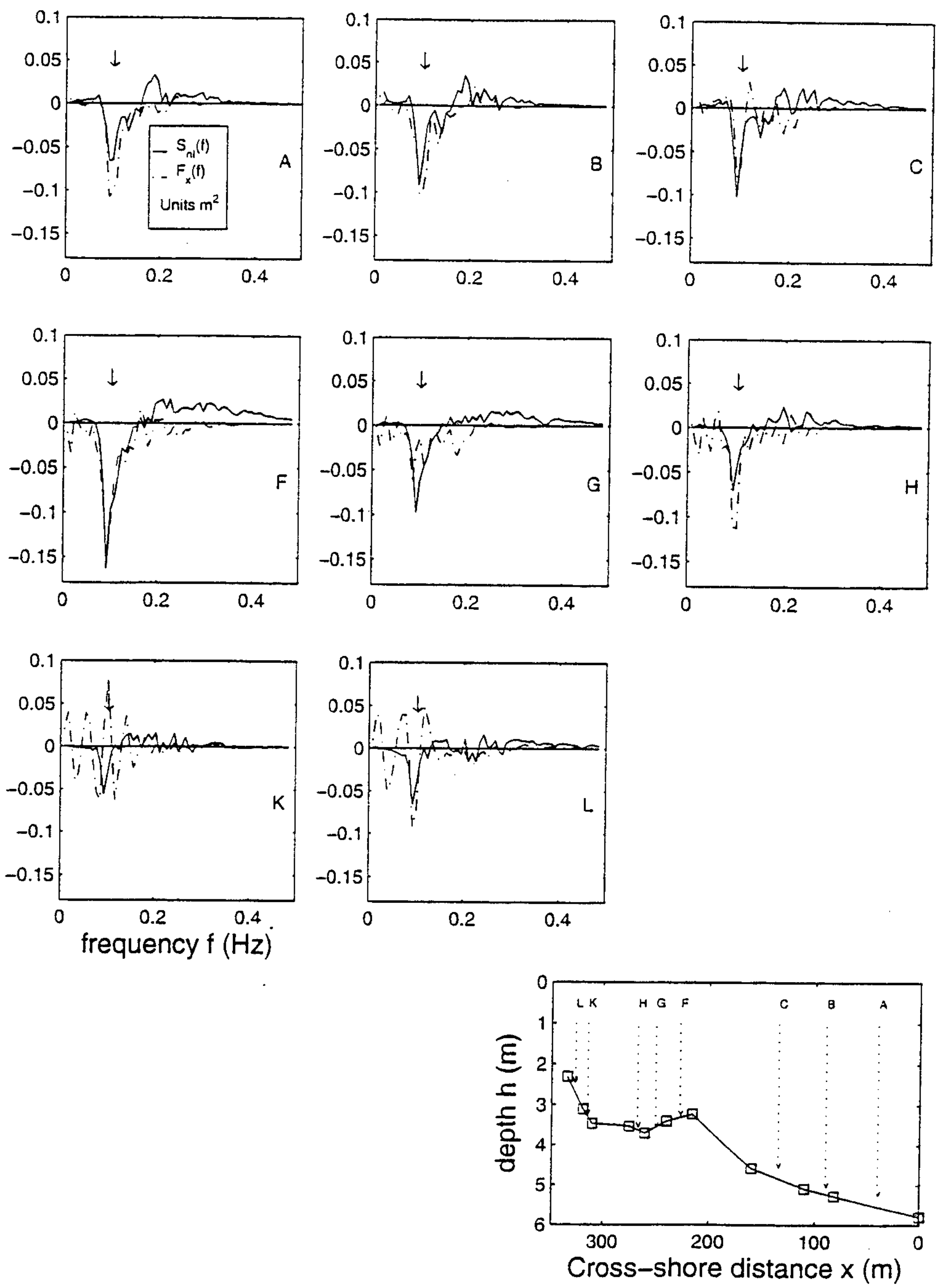

A
B
C
F
G
H
K
L
$S_{nl}(f)$
$F_x(f)$
Units m^2
frequency f (Hz)
depth h (m)
Cross-shore distance x (m)

Figure 7

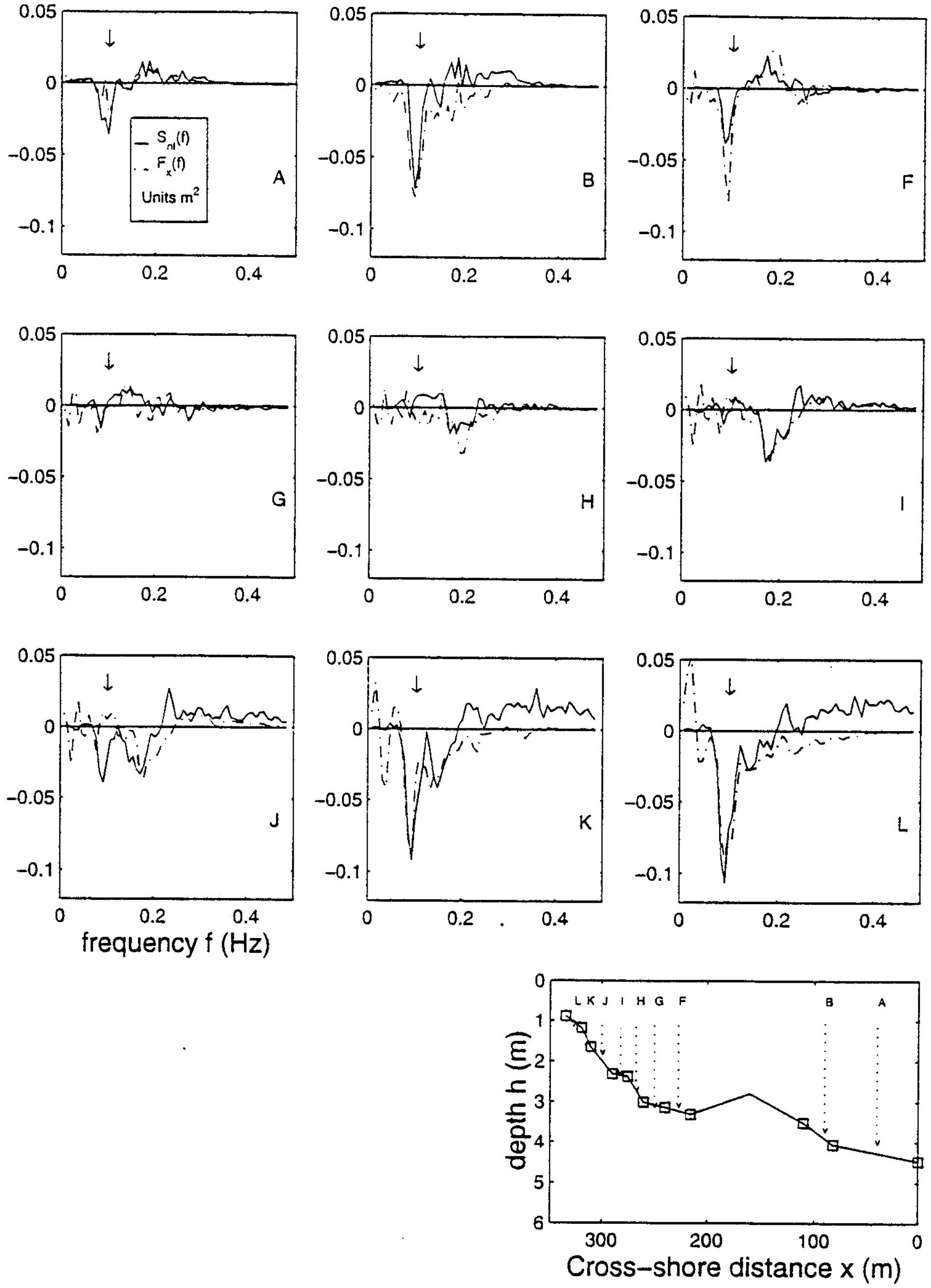

$S_{nl}(f)$
$F_x(f)$
Units m^2
A
B
F
G
H
I
J
K
L
frequency f (Hz)
L K J I H G F B A
depth h (m)
Cross-shore distance x (m)

Figure 8

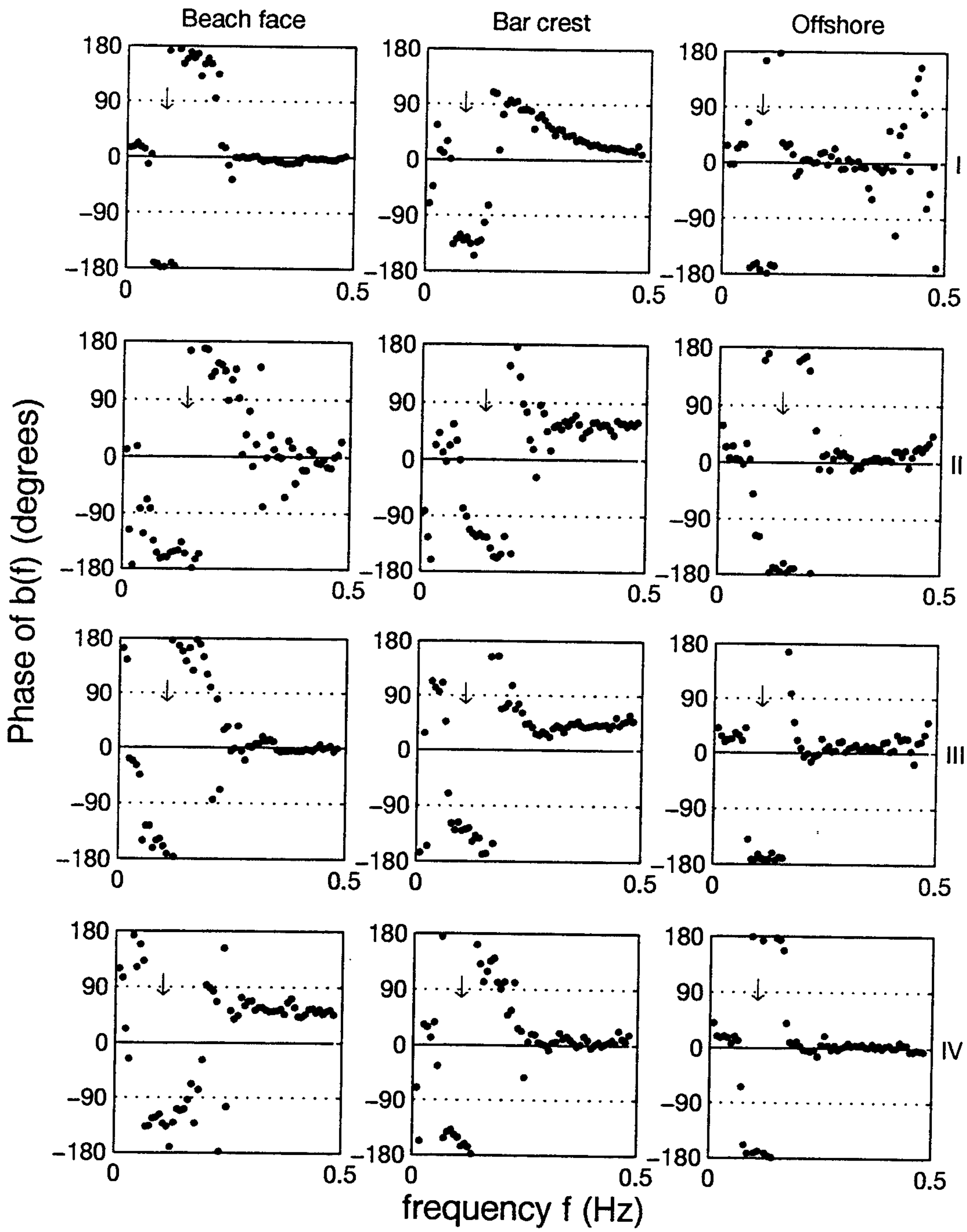

Beach face
Bar crest
Offshore
Phase of b(f) (degrees)
frequency f (Hz)
180
90
0
-90
-180
0
0.5
I
II
III
IV

Figure 9

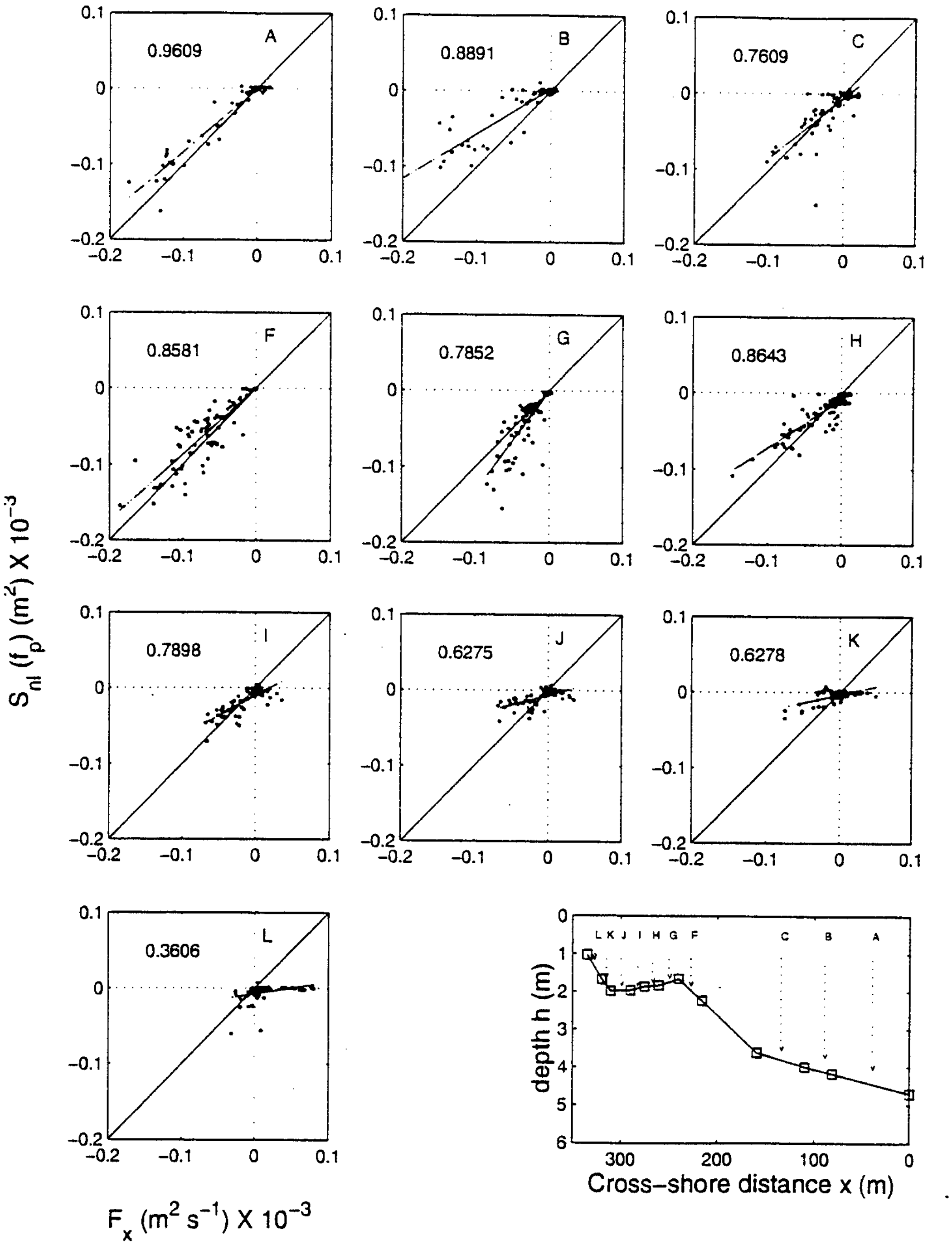
0.9609
A
0.8891
B
0.7609
C
0.8581
F
0.7852
G
0.8643
H
0.7898
I
0.6275
J
0.6278
K
0.3606
L
$S_{nl}(f_p)$ (m^2) X 10^{-3}
F_x $(m^2\ s^{-1})$ X 10^{-3}
depth h (m)
Cross-shore distance x (m)
L K J I H G F C B A

Figure 10

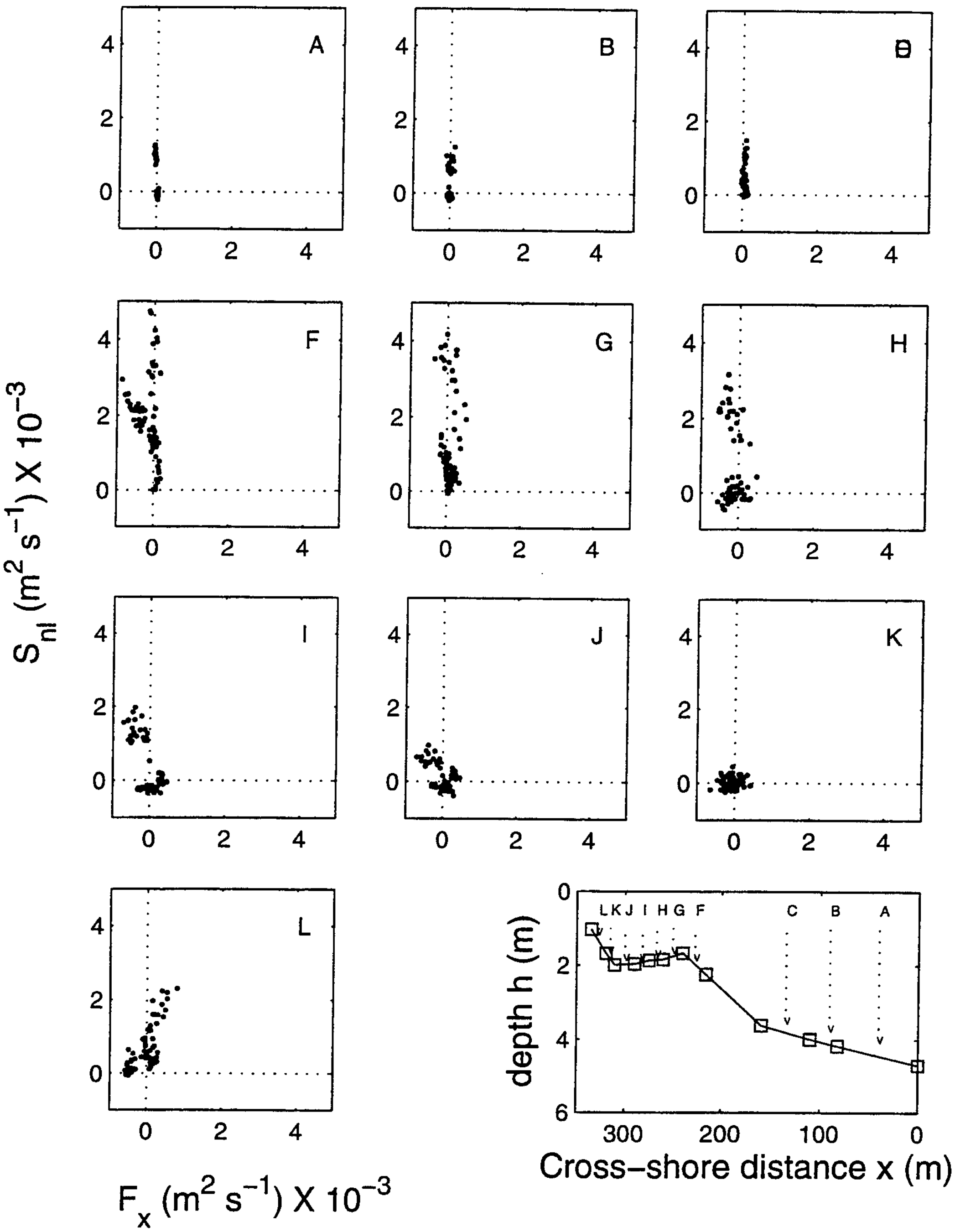
A
B
B
F
G
H
I
J
K
L
S_{nl} ($m^2 s^{-1}$) X 10^{-3}
F_x ($m^2 s^{-1}$) X 10^{-3}
L K J I H G F
C
B
A
depth h (m)
Cross-shore distance x (m)

Figure 11

LIST OF REFERENCES

Battjes, J. A., 1972, "Set-up due to irregular waves", *Proceedings of the 13th International Conference on Coastal Engineering.*, ASCE, 1993-2004.

Battjes, J. A. and J. P. F. M. Janssen, 1978, "Energy loss and set-up due to breaking of random waves, *Proceedings of the 16*th *International Conference on Coastal Engineering.*, ASCE, 569-587.

Battjes, J. A. and M.J.F. Stive, 1985," Calibration and verification of a dissipation model for random breaking waves", *J. Geophys. Res.*, 90, 9159-9167.

Chen, Y., and R.T. Guza, 1997, "Modeling spectra of breaking surface waves in shallow water, " *J. Geophys. Res.*, 102(C11), 25,035-25,046.

Collins, J. I., 1970, "Probabilities of breaking wave characteristics", *Proceedings of the 12th International Conference on Coastal Engineering.*, ASCE, 399-412.

Eldeberky, Y. and J.A. Battjes, 1996, "Spectral modeling of wave breaking: Application to Boussinesq equations". *J. Geophys. Res.*, 101, 1253-1264.

Elgar, S. and R.T. Guza, 1985b, "Observations of bispectra of shoaling surface gravity waves", *J. Fluid Mech.*, 161, 425-448.

Elgar, S., M.H. Freilich, and R.T Guza, 1990a, "Model-data comparisons of moments of nonbreaking shoaling surface gravity waves", *J. Geophys. Res.*, 95, 16055-16063.

Elgar, S., R.T. Guza, B. Raubenheimer, T.H.C. Herbers, and E. L. Gallagher, 1997, "Spectral evolution of shoaling and breaking waves on a barred beach. *J. Geophys. Res.*, 102, 15797-15805.

Freilich, M.H. and R.T. Guza, 1984, "Nonlinear effects on shoaling surface gravity waves", *Philos. Trans. R. Soc. London,* Ser. A311, 1-42.

Goda, Y., 1975, "Irregular wave deformation in the surf zone", *Coastal Eng, Jpn.*, 18, 13-26.

Hasselmann, K., W. Munk, and G. MacDonald, 1963, "Bispectra of ocean waves", Time Series Analysis, Chap. 8, John Wiley & Sons, Inc.

Herbers, T.H.C. and M.C. Burton, 1997, "Nonlinear shoaling of directionally spread waves on a beach", *J. Geophys. Res., 102,* 21101-21114.

Liu, P. L.-F., S. B. Yoon, and J. T. Kirby, 1985, "Nonlinear refraction-diffraction of waves in shallow water", *J. Fluid Mech.*, 153, 185-201.

Madsen, P. A., R. Murray, and O. R. SØrensen, 1991, "A new form of the Boussinesq equations with improved linear dispersion characteristics", *Coastal Engng*, 15, 371-388.

Mase, H., and J. T. Kirby, 1992, "Hybrid frequency-domain KdV equation for random wave transformation", *Proceedings of the 23rd International Conference on Coastal Engineering.*, ASCE, 474-487.

Norheim, C.A., T.H.C. Herbers, and S. Elgar, 1998, " Nonlinear evolution of surface wave spectra on a beach", *J, Phys. Oceanogr.,* in press.

Peregrine, D.H., 1967, "Long waves on a beach", *J. Fluid Mech.*, 27, Part 4, 815-827.

Thornton, E. B. and R.T. Guza, 1983, " Transformation of wave height distribution", *J. Geophys. Res.*, 88, 5925-5938.

Thornton, E. B., 1997,"Rederivation of the saturation range in the frequency spectrum of wind-generated gravity waves", *J. Phys. Oceanogr.*, 7, 137-140.

Thornton, E. B., 1979," Energetics of breaking waves within the surf zone", *J. Geophys. Res.*, 84, 4931-4938.

INITIAL DISTRIBUTION LIST

No. Copies

1. Defense Technical Information Center 2
   8725 John J. Kingman Rd., STE 0944
   Ft. Belvoir, VA 22060-6218

2. Dudly Knox Library 2
   Naval Postgraduate School
   411 Dyer Rd.
   Monterey, CA 93943-5102

3. Professor T.H.C. Herbers, Code OC/He. 6
   Department of Oceanography
   Naval Postgraduate School
   Monterey, CA 93943 - 5121

4. Professor E.B. Thornton, Code OC/Tm 1
   Department of Oceanography
   Naval Postgraduate School
   Monterey, CA 93943 - 5121

5. P.F. Jessen, Code Oc/Js 1
   Department of Oceanography
   Naval Postgraduate School
   Monterey, CA 93943-5121

6. Tom Lippmann 1
   Center for Coastal Studies, 0209
   Scripps Institute of Oceanography
   University of California, San Diego
   La Jolla, CA 92093-0209

7. LCDR Noel Russnogle 2
   2022 S.E. Eagle
   Gresham, OR 97080